10-28-2015

The Corpus Callosum in Primates: Processing Speed of Axons and the Evolution of Hemispheric Asymmetry

Kimberley A. Phillips
Trinity University, kphilli1@trinity.edu

Cheryl D. Stimpson

J. B. Smaers

Mary Ann Raghanti

B. Jacobs

See next page for additional authors

Publication Details

Proceedings of the Royal Society B: Biological Sciences

PROCEEDINGS B

rspb.royalsocietypublishing.org

Research

Cite this article: Phillips KA, Stimpson CD, Smaers JB, Raghanti MA, Jacobs B, Popratiloff A, Hof PR, Sherwood CC. 2015 The corpus callosum in primates: processing speed of axons and the evolution of hemispheric asymmetry. *Proc. R. Soc. B* **282**: 20151535. http://dx.doi.org/10.1098/rspb.2015.1535

Received: 24 June 2015
Accepted: 1 October 2015

Subject Areas:
evolution, neuroscience

Keywords:
conduction velocity, axons, interhemispheric communication, corpus callosum

Author for correspondence:
Kimberley A. Phillips
e-mail: kimberley.phillips@trinity.edu

The corpus callosum in primates: processing speed of axons and the evolution of hemispheric asymmetry

Kimberley A. Phillips[1,2], Cheryl D. Stimpson[3], Jeroen B. Smaers[5], Mary Ann Raghanti[6], Bob Jacobs[7], Anastas Popratiloff[4], Patrick R. Hof[8] and Chet C. Sherwood[3]

[1]Department of Psychology, Trinity University, San Antonio, TX 78212, USA
[2]Southwest National Primate Research Center, Texas Biomedical Research Institute, San Antonio, TX, USA
[3]Department of Anthropology and Center for the Advanced Study of Human Paleobiology, and [4]Center for Microscopy and Image Analysis, The George Washington University, Washington, DC, USA
[5]Department of Anthropology, Stony Brook University, Stony Brook, NY, USA
[6]Department of Anthropology and School of Biomedical Sciences, Kent State University, Kent, OH, USA
[7]Department of Psychology, Colorado College, Springs Colorado, CO, USA
[8]Fishberg Department of Neuroscience and Friedman Brain Institute, Icahn School of Medicine at Mount Sinai, New York, NY, USA

Interhemispheric communication may be constrained as brain size increases because of transmission delays in action potentials over the length of axons. Although one might expect larger brains to have progressively thicker axons to compensate, spatial packing is a limiting factor. Axon size distributions within the primate corpus callosum (CC) may provide insights into how these demands affect conduction velocity. We used electron microscopy to explore phylogenetic variation in myelinated axon density and diameter of the CC from 14 different anthropoid primate species, including humans. The majority of axons were less than 1 µm in diameter across all species, indicating that conduction velocity for most interhemispheric communication is relatively constant regardless of brain size. The largest axons within the upper 95th percentile scaled with a progressively higher exponent than the median axons towards the posterior region of the CC. While brain mass among the primates in our analysis varied by 97-fold, estimates of the fastest cross-brain conduction times, as conveyed by axons at the 95th percentile, varied within a relatively narrow range between 3 and 9 ms across species, whereas cross-brain conduction times for the median axon diameters differed more substantially between 11 and 38 ms. Nonetheless, for both size classes of axons, an increase in diameter does not entirely compensate for the delay in interhemispheric transmission time that accompanies larger brain size. Such biophysical constraints on the processing speed of axons conveyed by the CC may play an important role in the evolution of hemispheric asymmetry.

1. Introduction

As brain size expands, the length over which axons must travel increases. Consequently, communication between the cerebral hemispheres may be constrained in larger brains as transmission delays rise with axon lengths. The speed of action potential propagation limits the flow of information within the nervous system and the ability for synchronization of activity among spatially dispersed brain regions [1]. Two possible solutions for improving the conduction velocity of action potentials are to increase the diameter of the axon and to add myelination [2,3]. It has been noted that axon diameters cannot scale at the same rate as increases in brain size, as this would require a prohibitively large expansion of white matter volume [4]. Therefore, it would be advantageous for a relatively small subset of faster conducting, larger diameter myelinated axons to counter the delay in transmission time that occurs owing to increased distances as brain

THE ROYAL SOCIETY PUBLISHING

Table 1. List of individuals, axon diameter (median and the largest diameter axons) and estimated cross-brain conduction times of fibres of the corpus callosum. (Data are for the average of all corpus callosum regions sampled. All brains were removed and immersion fixed in 10% buffered formalin after variable postmortem intervals, which never exceeded 15 h.)

				axon diameter (μm)		estimated cross-brain conduction time (ms)	
species	sex	age (years)	brain mass (g)	median	95th percentile	median	95th percentile
Homo sapiens	F	45	1250	0.62	2.88	37.52	8.13
Homo sapiens	M	54	1625	0.93	3.43	27.56	7.47
Gorilla gorilla	M	49	477	0.68	2.26	24.91	7.55
Pan paniscus	M	34	313	0.48	1.72	30.82	8.56
Pan troglodytes	M	31	407	0.59	1.96	27.35	8.23
Pongo pygmaeus	M	33	287	0.60	2.06	23.88	6.95
Symphalangus syndactylus	F	17	107	0.53	1.80	19.47	5.72
Cercocebus agilis	F	19	95	0.43	1.41	22.86	7.06
Colobus guereza	F	15	84	0.52	2.16	18.45	4.42
Macaca nemestrina	F	7	86	0.44	1.38	21.70	6.96
Papio hamadryas	F	31	140	0.53	1.78	21.36	6.34
Alouatta caraya	M	21	56	0.62	1.80	13.38	4.61
Pithecia pithecia	F	1	30	0.52	1.92	12.96	3.53
Saguinus geoffroyi	M	15	11	0.43	1.74	11.18	2.74
Saimiri sciureus	F	27	19	0.43	1.20	13.63	4.86

size expands. Larger brains might be expected to have relatively thicker axons at the upper end of the size distribution than smaller brains, although spatial packing constraints limit the rate at which these types of connections can increase.

The corpus callosum (CC) provides the major white matter link between the two cerebral hemispheres, with more than 300 million fibres connecting homotopic and heterotopic cortical regions in humans [5]. Small diameter (less than 2 μm), lightly myelinated fibres are found mainly in the anterior and posterior regions connecting higher-order association areas, whereas larger diameter fibres (greater than 2 μm) predominate in the middle regions connecting primarily motor and somatosensory areas [6,7] and in the posterior region for visual callosal axons [8–10]. Increased density of axons is also found towards the middle and posterior portion of the CC [5].

The diameter of CC axons is related to conduction speed [11–13]. Unmyelinated axons are compact and slow conducting, whereas myelinated axons are larger and faster conducting [14]. As brain size increases, conduction delay is expected to rise as a function of distance. Minimizing conduction delay is crucial for time-sensitive information such as sensation and perception, as well as the function of neuronal networks that depend on synchronized spike-time arrival and oscillator coupling [15], but rapid conduction is costly in terms of increased brain volume. Ringo *et al.* [4] suggested that conduction delays in large brains were too long to support complex, time-critical computations, leading to the modularization of these processes into specialized local lateralized networks in large brains. As a result, functional lateralization is expected to emerge as brain size expands. Improving the conduction velocity for interhemispheric signalling can be accomplished by having a significant subset of larger-diameter axons. In a comparative study of the splenium in shrew, mouse, rat, cat, marmoset and macaques, Wang *et al.* [16] showed that the widest callosal axons (greater than 2 μm) increased in size with brain diameter, but that unmyelinated axons and narrower myelinated axons did not. Across all species the fastest interhemispheric conduction times conveyed by the largest axons were maintained at less than 5 ms [16].

Previous studies of CC axon distributions have included samples from either a relatively small number of species [8,17–19], a restricted region of the CC [20], or a broad comparative assembly of phylogenetically distant relatives [16]. To our knowledge, no investigation of axon size distributions among different regions of the CC has been conducted with a representative sample of species across primate phylogeny. Determining characteristics of axon size distributions within the CC and its subdivisions in primates may shed light on how these demands impact conduction speed and have been balanced in brain evolution. To address these issues, we studied phylogenetic variation in axonal density and diameter of the CC across 14 different anthropoid primate species.

2. Material and methods

The sample included New World monkeys ($n = 4$), Old World monkeys ($n = 4$), apes ($n = 5$) and humans ($n = 2$) (table 1). The phylogeny of the species used is based on the consensus tree from the 10 k trees website (figure 1) [21]. Non-human brains were provided by American Zoo and Aquarium-accredited zoos or research institutions, and all animals were maintained in accordance with Federally recognized standards, guidelines and principles. All subjects, except *Macaca maura*, died of natural

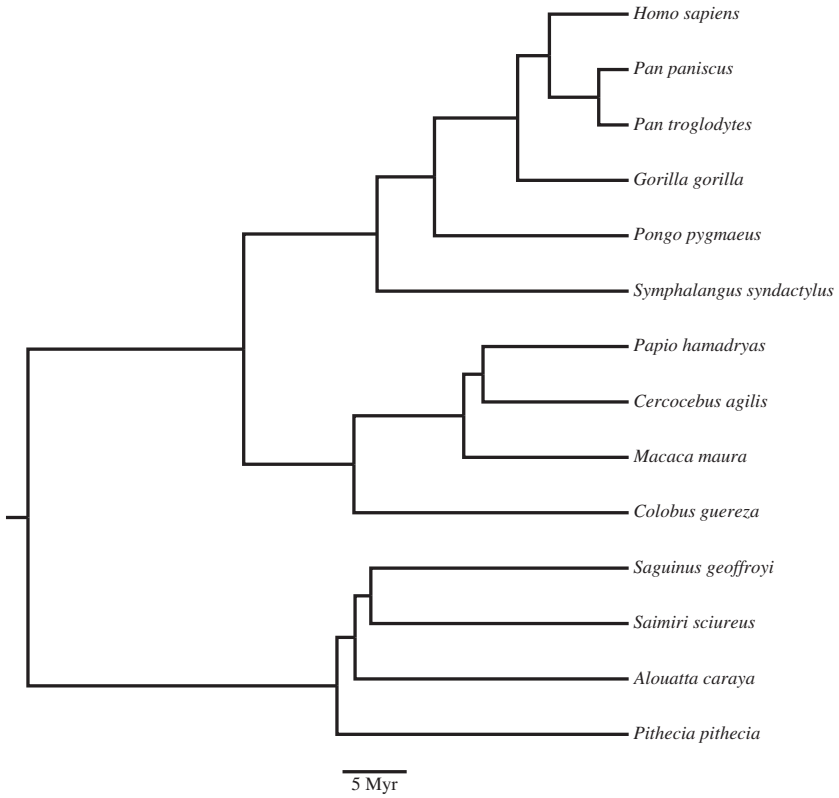

Figure 1. The phylogeny of the species used, based on the consensus tree from the 10 k trees website.

causes; the macaque subject was part of another non-neurological research study, and as part of that protocol was perfused. None of the brains included in this study showed gross abnormalities or pathology on veterinary inspection. All brains were immersion fixed in 10% buffered formalin after variable postmortem intervals, which never exceeded 14 hours. Human brains were collected at autopsy from the El Paso county coroner's office in Colorado Springs, in accordance with Colorado College Institutional Review Board (no. 011311-1). These individuals died from non-neurological causes. The brains were removed and immersion fixed in 10% buffered formalin 14 (female) or 15 (male) h after death. After an initial period of fixation, brains were transferred into a 0.1 M phosphate-buffered saline (pH 7.4) solution containing 0.1% sodium azide and stored at 4°C.

Brain masses of non-human specimens were measured either immediately after perfusion or directly upon receipt from the donating institution. Human brain masses were measured at autopsy. Some artefact in the measures of total brain mass in the sample owing to interindividual differences in fixation length was unavoidable. Nevertheless, shrinkage artefact is likely to be minimal, because brain mass measurements in the sample fall close to the normal range of values reported in the literature for fresh brains from these taxa [22–24].

The CC from each specimen was sectioned in the midsagittal plane. The CC was subdivided into five regions, following Witelson [6] (figure 2). Although there are more recent parcellations of the CC for rhesus monkeys and humans [19,25,26] based on diffusion tensor imaging, it is not certain that these can be generalized across all primates.

A 1 × 4 mm section was cut from the centre of each subdivision and placed into a microcentrifuge tube containing 1% glutaraldehyde and 4% paraformaldehyde, for a period of at least one week. Samples were prepared for transmission electron microscopy using a modified technique for processing nerve biopsies. Samples were postfixed in 1% Zetterqvist's buffered osmium tetroxide, dehydrated, infiltrated with resin and embedded before sectioning. Semithin sections were first cut and then stained with toluidine blue and examined under a light microscope to verify correct orientation before continuing. Subsequent ultrathin silver sections were mounted on electron microscopic grids and stained with uranyl acetate before viewing under the electron microscope.

Axon density and diameter were determined from electron micrographs from 6000× digital images taken by a digital camera coupled to a JOEL JEM 1200EX electron microscope. An average of 34 images was acquired from each CC subdivision from each subject. Counts and measurements of axon diameter were made over a 100 × 200 μm^2 region in each micrograph in a systematic-random fashion using fractionator sampling implemented in the National Institutes of Health ImageJ. We analysed myelinated axons only because they could be identified unambiguously in these samples. Axon diameter was defined as the average of the fitted major and minor axis lengths for major–minor ratios less than 1.5, and otherwise as the minor axis. The individual performing these measures (C.D.S.) was blind to the species and region of each sample. A mean of 397 (s.d. = 69) axons were counted and measured in each CC region of each specimen.

(a) Data analysis

To determine the scaling relationships we employed phylogenetic generalized least-squares (PGLS) regression with a likelihood-fitted lambda transformation. If a standard regression is used with comparative data, the slope drawn through closely related species may appear to be shallower than the slopes drawn through distantly related species [27]. To correct for this, the statistical method must take into account the expected error structure given the phylogenetic relatedness of the species studied. PGLS incorporates this error structure by weighting observations according to a variance–covariance matrix of relative phylogenetic distance between species. PGLS is thus a standard regression in which the estimates of the scaling coefficients are calculated based on weighted observations [28]. The variance–covariance matrix of phylogenetic relatedness

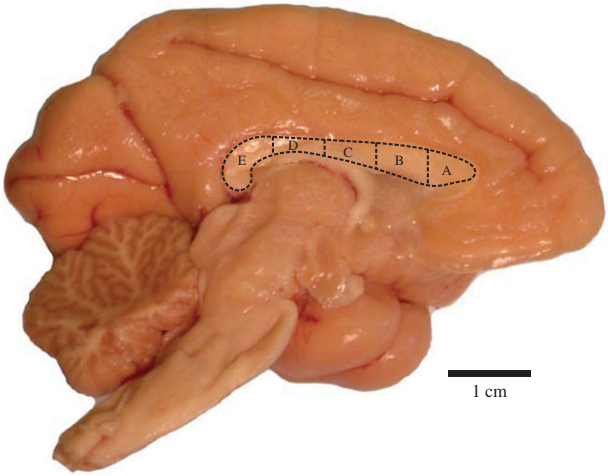

Figure 2. The corpus callosum of a mantled guereza (*Colobus guereza*), indicating the five regional subdivisions (A–E). (Online version in colour.)

is further adjusted for the extent to which the data adhere to a pure gradual model of evolution using a likelihood-fitted lambda transformation. Lambda varies between zero and unity, where zero indicates that traits covary independently of their degree of shared ancestry, and unity indicates that traits covary in a manner accurately described by their degree of shared ancestry. In practice, the lambda transformation multiplies the off-diagonal elements in the variance–covariance matrix of phylogenetic relatedness to the value of lambda to produce the variance–covariance structures that best describe how traits covary in relation to their degree of shared ancestry. When zero is unity, PGLS is therefore equivalent to a standard generalized least-squares (GLS) regression. PGLS confidence intervals were calculated according to Rohlf [28]. In order to facilitate interpretation of allometric slopes from regressions of axon diameters versus brain mass, we used the cube root of brain mass to bring it into a similar geometric dimensionality as the linear measures of axon diameter.

Conduction velocities were calculated as $v = 5.7{*}D$ for myelinated axons, where v is in $\mathrm{m\,s^{-1}}$ and D is the outer axon diameter in μm [11]. Cross-brain conduction times were then calculated as v*brain diameter. Brain diameters were calculated as the diameter of the sphere of reported brain mass (table 1).

3. Results

Examples of electron micrographs of CC tissue can be seen in figure 3. As expected, there was a wide range of axon diameters present in all species. The majority of myelinated axons in our sample were less than 1 μm in diameter (median diameter = 0.56 μm; table 1 and figure 4). The distribution of axon diameters in all species showed positive skew (figure 5).

To examine the differential scaling of the most common axon diameters compared with the largest axons, we calculated the median and 95th percentile from axon diameter distribution for each CC region. To represent the axon diameters and density across the entire CC in each specimen, we used the average of all CC region measurements. Table 2 displays the PGLS coefficients for axon scaling in the sample regressed against brain mass.

There were no significant differences among CC regions for the scaling of either median or 95th percentile axon diameters versus brain mass (i.e. all the slopes were contained within the 95% intervals of the other CC regions). Axons within the different regions of the CC changed in diameter at a similar rate with variation in brain size, regardless of their anterior–posterior location. Thus, the scaling slope of the whole CC axon diameter measurements can be taken to represent the manner in which axons change relative to brain mass across anthropoid primates. The scaling slope of median axon diameter in the whole CC was 0.18 (95% confidence intervals (CIs) = 0.07–0.28; $r^2 = 0.53$, $p < 0.001$, lambda = 0.4) and the scaling slope of the 95th percentile axon diameter was 0.15 (95% CIs = 0.04–0.27; $r^2 = 0.41$, $p = 0.01$, lambda = 0; figure 6). These slopes indicate a negative allometric relationship between axon diameters of the CC and brain mass such that increases in axon diameter do not match the rate of brain size enlargement. In this sample, brain mass varied by 97-fold with only a 1.8-fold difference in median axon diameters between the largest (*Homo*) and smallest (*Saguinus* and *Saimiri*) brains and a 2.1-fold difference in the diameters of axons in the 95th percentile.

As another way of examining the scaling of axon diameters, we also regressed the 95th percentile axons on the median directly (figure 7). Within each CC region, the 95th percentile diameter of axons correlated significantly with the median diameter. The scaling slopes progressively increased from regions A to E (A, 0.697; B, 0.744; C, 0.917; D, 1.267; E, 1.337), but with CIs that always include isometry. The scaling coefficients of regions A and B were significantly ($p < 0.05$) lower than those of regions D and E (95% CIs of the scaling coefficients: A, 0.292–1.102; B, 0.229–1.258; C, 0.564–1.270; D, 0.653–1.880; E, 1.940–1.734). The likelihood-estimated lambda value for all these regressions was zero, suggesting that the median and 95th percentile diameter of axonal thickness does not covary in tandem with phylogenetic relatedness.

Concomitant with increased axon diameters that are associated with greater brain size, axon density in the CC also tended to decrease (figure 6). The scaling slope of axon density in the whole CC was −0.44 (95% CIs = −0.78 to −0.09; $r^2 = 0.39$, $p = 0.02$, lambda = 0) and was illustrated by a 2.8-fold difference in total axon density between the largest and the smallest brains in the sample. Axon density scaling relative to brain mass did not significantly differ across the regions of the CC (table 2 and figure 6).

Finally, to determine the implications of cross-species variation in the size of CC axons, we estimated the interhemispheric conduction time for an action potential. The conduction time of the 95th percentile of diameter thickness correlated significantly with overall brain size in regions A, D and E (A, $r^2 = 0.500$; $p = 0.005$; D, $r^2 = 0.457$, $p = 0.008$; E, $r^2 = 0.670$, $p = 0.0003$) but not in regions B and C. In each instance, the direction of the correlation was negative. Our estimates of the fastest cross-brain conduction times, as conveyed by axons at the 95th percentile, varied within a narrow range (3–9 ms) across species, whereas the cross-brain conduction times for the median axon diameters differed more significantly among species (11–38 ms). Nonetheless, even with a compensatory increase in axon diameter, interhemispheric transmission times tended to rise with larger brain size (figure 8).

4. Discussion

We provide here a comparative quantitative examination of myelinated axons of the CC in anthropoid primates, including humans. Results indicate that the distribution of axon diameters displayed positive skew in all species examined with a median in the total sample that was less than 1 μm. Similar

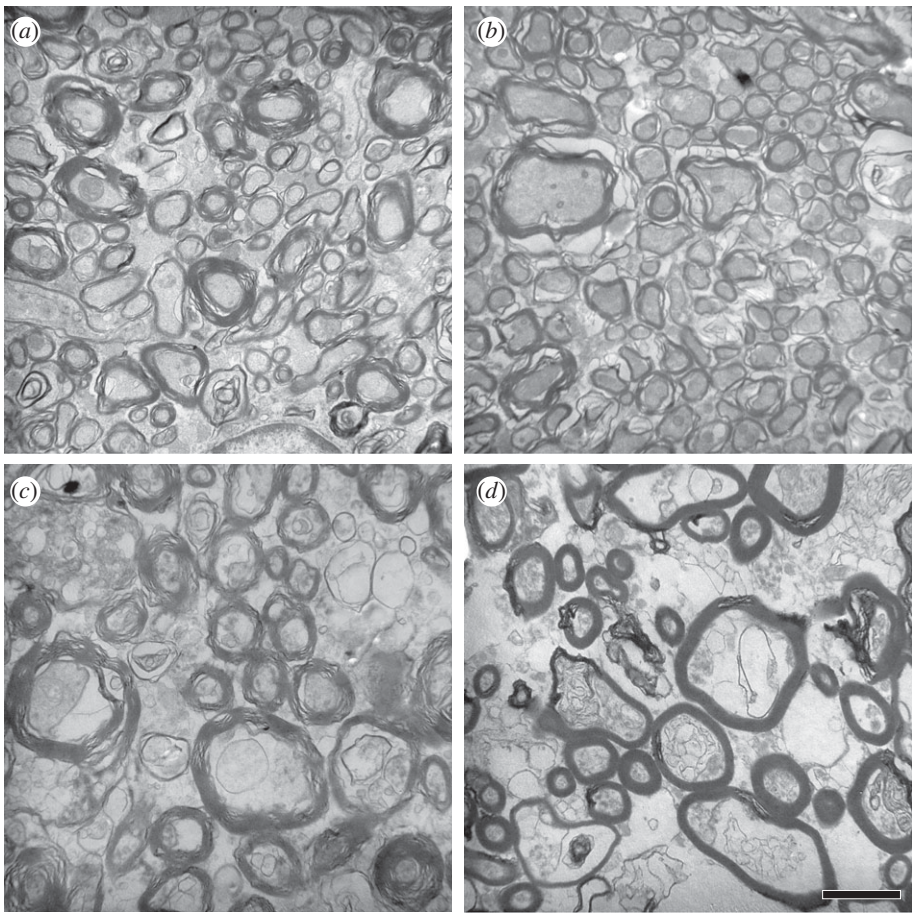

Figure 3. Electron micrographs of callosal tissue from subdivision E from (*a*) *Saimiri sciureus*, (*b*) *Macaca maura*, (*c*) *Gorilla gorilla* and (*d*) *Homo sapiens*. Scale bar, 1 µm.

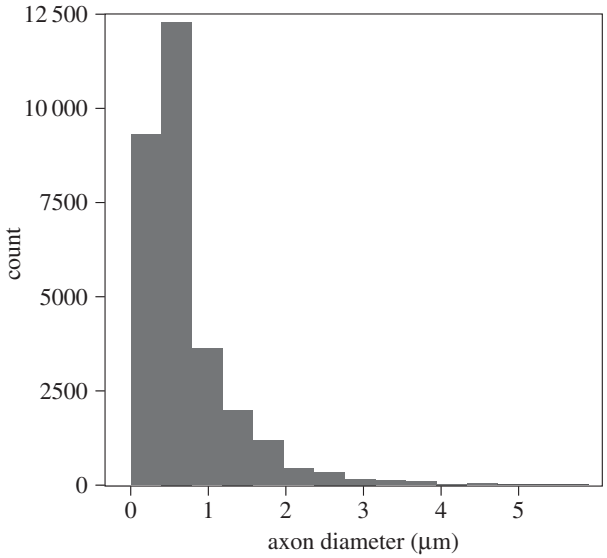

Figure 4. Frequency histogram of axon diameters across the entire sample of species. The most frequently occurring axons are 0.5 µm; axons are rarely larger than 2 µm.

results have been reported for the myelinated fibres in the CC of humans [1,5] and macaque monkeys [17,18]. We also found that axons within the different regions of the CC changed in diameter at a similar rate with variation in brain size, regardless of their anterior–posterior location. Previous cross-species studies have tended to sample just one CC region and did not test whether there are differences across the anterior–posterior axis. It is notable that we did not find significant scaling differences from CC regions as divergent as the genu and splenium. Furthermore, as brain size increased and axon diameters became larger, axon density in the CC decreased. Finally, interhemispheric conduction times were found to increase for the median diameter axons in association with brain size much more rapidly than for the largest axons. These results have implications for understanding the effects of evolutionary changes in brain size in primates on neural processing speed and hemispheric lateralization.

Our findings show that as brain size increases, conduction delay rises as a function of distance. These findings confirm and extend previous studies conducted on domestic mammals and primates [8,16,29,30]. With increasing brain size, a small subset of axon fibres become disproportionately larger with increased conduction velocity. However, the enlargement of axon diameters may not be great enough to compensate for the increased interhemispheric distance in larger brains. As a result, the speed of action potential signalling across the brain via the CC is relatively delayed, which might cause the degree of interhemispheric connectivity to be reduced. These factors could promote the evolution of hemispheric specialization in correlation with the enlargement of brain size [4,31,32]. Indeed, in our sample of anthropoid primates, smaller brains were found to have shorter cross-brain conduction times than larger brains. Our data further indicate that the fastest interhemispheric conduction times (less than 10 ms) are provided by only a few large myelinated axons conveyed by the CC. These largest diameter axons allow for the velocity of some

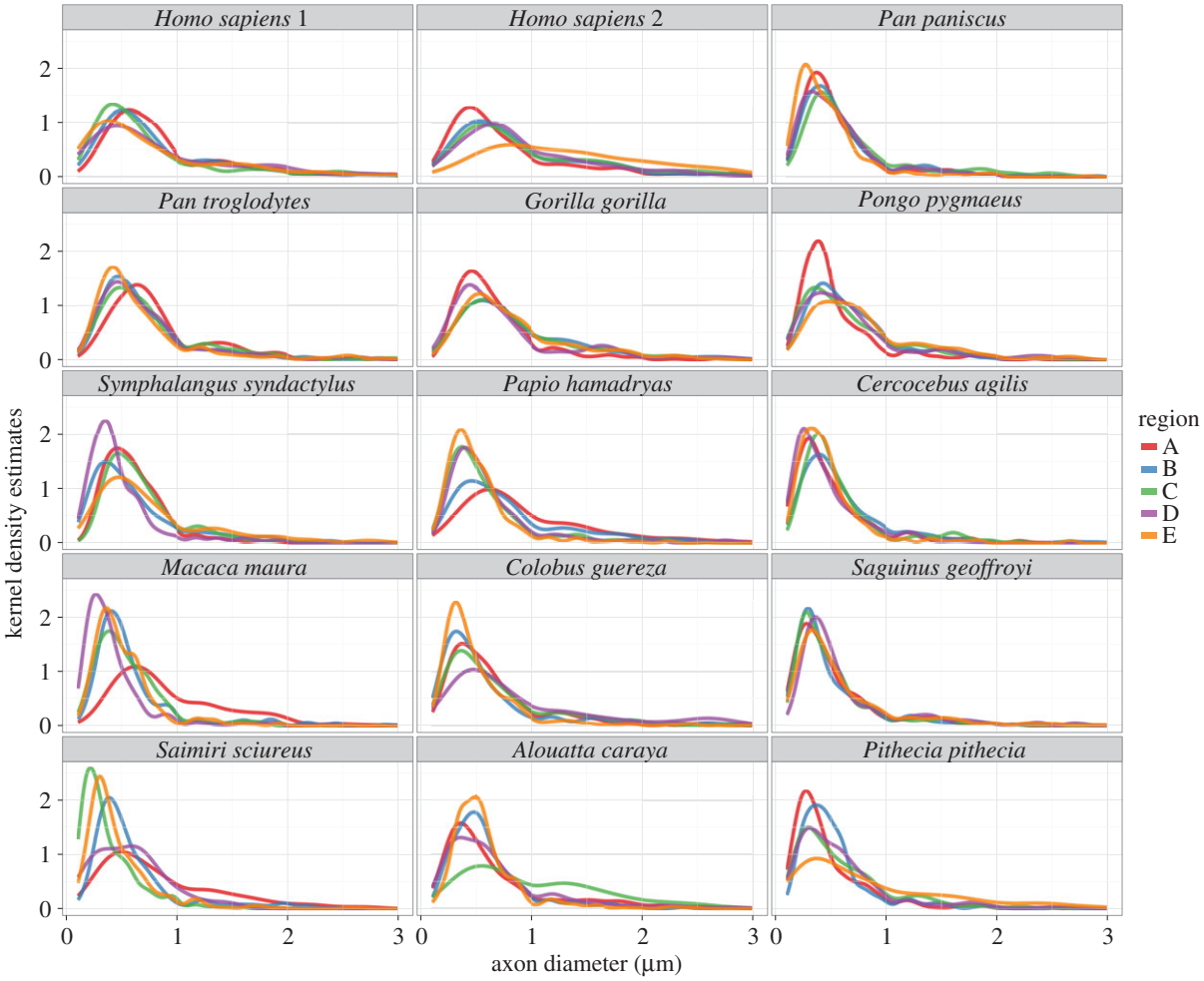

Figure 5. Kernel density estimation plot of axon diameters in each species according to CC subdivision (A–E). Plots are truncated at 3 µm as extremely small numbers of axons were larger than this in all species examined.

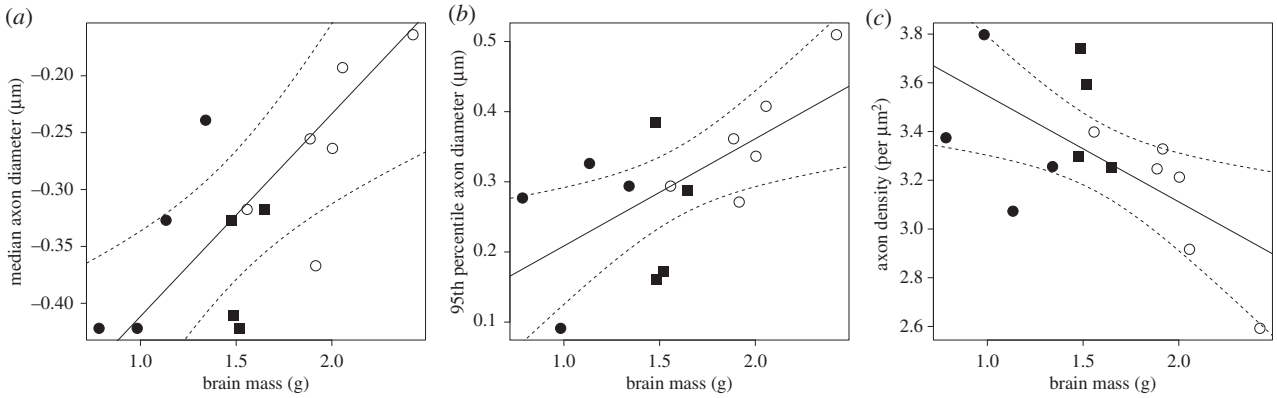

Figure 6. (*a*) Median callosal axons regressed against brain mass; (*b*) 95th percentile callosal axons regressed against brain mass; (*c*) axon density regressed against brain mass. Dashed lines are confidence intervals. Solid circles, New World monkeys; solid squares, Old World monkeys; open circles, hominoids.

neural signals to be kept relatively constant across brain size [32]. Similarly, Caminiti *et al*. [19] concluded that axon diameter is more important to restrict conduction delays to a minimum for interhemispheric connectivity than is the length of callosal axon bundles.

Axons of various diameters originate from different cortical areas in macaques [9,30], indicating that there is variability in the effect of conduction delays as signals converge on their targets at different times [19,30]. Caminiti *et al*. [19] showed that axon diameter increased with axonal length, however this relationship was not sufficient to maintain equivalent conduction velocities across the hemisphere. While the slowest conduction velocities occurred in the prefrontal regions, and the faster conduction velocities occurred in motor, somatosensory and visual areas, there was considerable variation in conduction velocity for all areas [19]. The present results, which showed a large range in axon diameters in all regions of the CC, also suggest that primates show great variability in interhemispheric transmission speed. It is possible that variability in cross-brain conduction times for information

Table 2. PGLS coefficients for axon measurements in the sample regressed against brain mass.

		95% CIs				
	slope	min.	max.	R^2	*p*	lambda
median axon diameter versus brain mass						
whole CC	0.18	0.07	0.28	0.53	0.00	0.40
region A	0.09	−0.08	0.26	0.10	0.27	0.00
region B	0.17	0.09	0.24	0.65	0.00	0.00
region C	0.17	0.02	0.33	0.33	0.03	0.00
region D	0.10	−0.04	0.23	0.17	0.14	0.00
region E	0.19	0.02	0.35	0.32	0.03	0.00
95th percentile axon diameter versus brain mass						
whole CC	0.15	0.04	0.27	0.41	0.01	0.00
region A	0.09	−0.07	0.25	0.10	0.26	0.00
region B	0.15	0.03	0.26	0.40	0.01	0.00
region C	0.22	0.07	0.37	0.46	0.01	0.00
region D	0.18	−0.04	0.39	0.21	0.10	0.00
region E	0.17	−0.11	0.46	0.13	0.21	0.00
axon density versus brain mass						
whole CC	−0.44	−0.78	−0.09	0.39	0.02	0.00
region A	−0.84	−1.69	0.00	0.28	0.05	1.00
region B	−0.55	−1.03	−0.07	0.34	0.03	0.00
region C	−0.55	−1.20	0.11	0.22	0.09	0.00
region D	−1.00	−2.12	0.11	0.24	0.07	1.00
region E	−0.28	−1.38	0.82	0.02	0.59	0.00
95th percentile axon diameter versus median axon diameter						
whole CC	1.06	0.65	1.47	0.72	0.00	0.00
region A	0.70	0.29	1.10	0.54	0.00	0.00
region B	0.74	0.23	1.26	0.45	0.01	0.00
region C	0.92	0.56	1.27	0.73	0.00	0.00
region D	1.27	0.65	1.88	0.63	0.00	0.00
region E	1.34	0.94	1.73	0.82	0.00	0.00

processing reflects the capacity to synchronize the activity of neuron assemblies across cortical regions and between the hemispheres. Perge *et al*. [33] note that larger axon diameters improve timing precision and provide higher information rates. Our data suggest that a variety of conduction velocities are required for interhemispheric communication and that variation in axon diameter is a reflection of the differences in the functional roles of these axons and the cortical regions they connect.

In each species, the largest diameter axons comprised a small proportion of the total number present, suggesting that they perform highly specific functions. Although the largest axons (those at the 95th percentile) and the median diameter axon scaled to brain mass similarly across the anterior–posterior axis of the CC, the largest axons increased in diameter progressively relative to the median axons towards the posterior region of the CC. The posterior region of the CC includes the splenium which is involved in synchronizing visual information between the two hemispheres [34]. Recent neuroimaging studies in humans suggest that different regions within the splenium provide interhemispheric connectivity of dorsal visual and association parietal areas, posterior cingulate and retrosplenial cortices, and ventral visual areas [20,35,36]. Thus, the importance of more rapid conduction times for visuospatial information may reflect the need to preserve the interhemispheric integration of such information.

Overall, the findings of this study support a model of brain scaling that predicts increases in brain size imposes biological limits to information processing which lead to the compartmentalization of wiring within lateralized local networks [37]. The transmission time of axons in the CC of anthropoid primates rises significantly as a function of brain size. The effects of axon dimension scaling impact all regions of the CC and lead to conduction delays that become more pronounced for the majority of axons as brain size expands. Even the largest axons do not increase in diameter to a

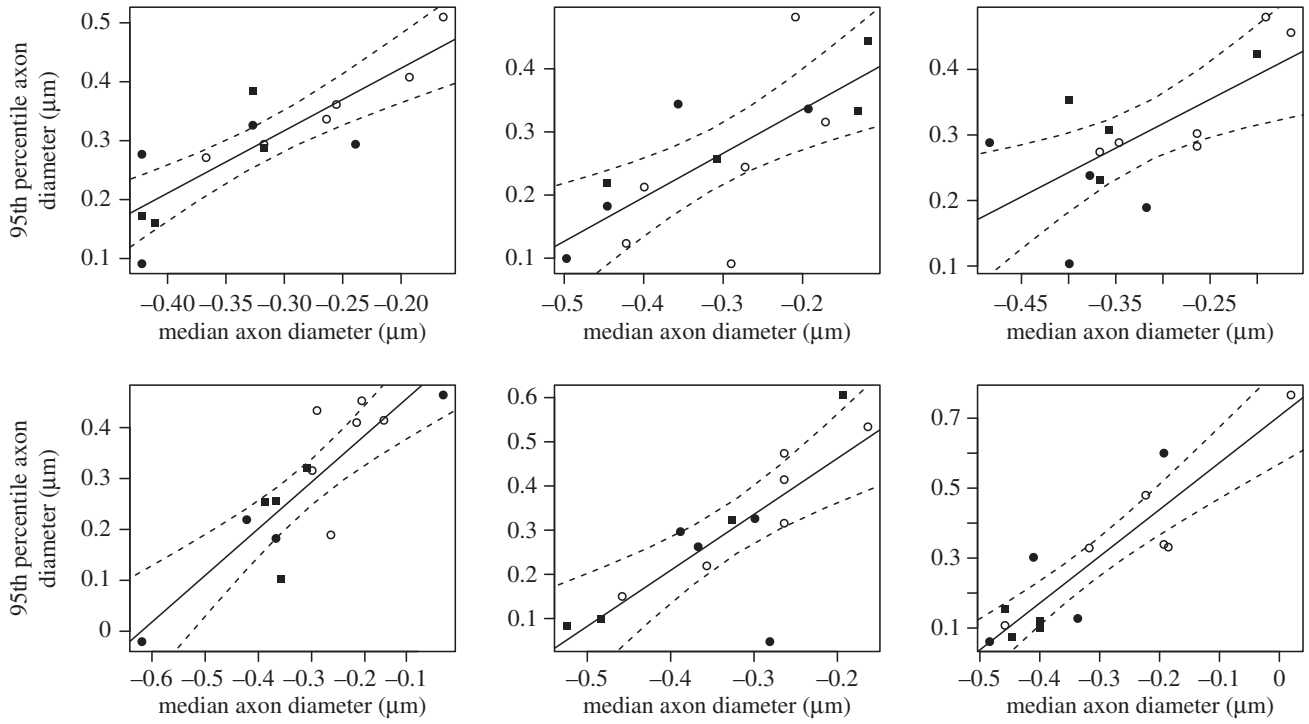

Figure 7. Callosal axons at the 95th percentile regressed on axons at the median. Solid circles, New World monkeys; solid squares, Old World monkeys; open circles, hominoids.

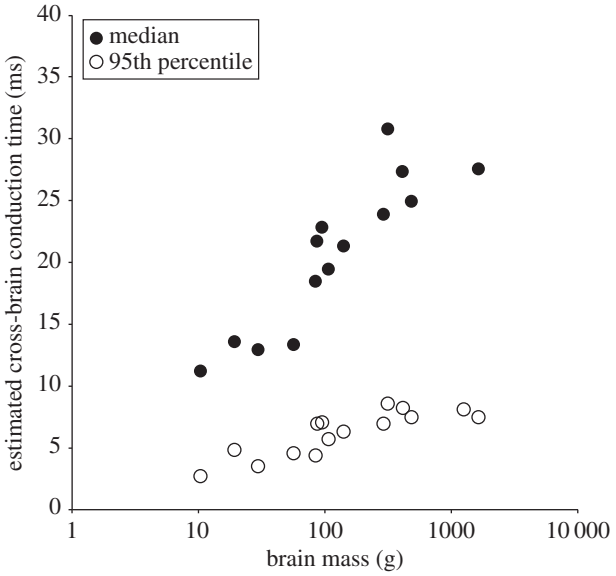

Figure 8. Estimated interhemispheric conduction times increased with larger brain sizes. Axons at the 95th percentile diameter provided the shortest interhemispheric conduction times.

sufficient degree to entirely compensate for the accumulation of longer spike transmission time with increasing brain mass. These results suggest that in large-brained species, such as great apes and humans, synchronized spike-time arrival for the transfer of information between hemispheres is a significant challenge. These dynamics might explain why functions that depend on precise timing, such as the multisensory perception of vocal communication and gestures [38] and control of the hand will display hemispheric lateralization in function that becomes more apparent with brain enlargement.

Ethics. All animals were maintained in accordance with Federally recognised standards, guidelines and principles.

Data accessibility. The dataset associated with this study is provided in table 1 and figures 4 and 5.

Authors' contributions. K.A.P. and C.C.S. conceived of the study, designed the study and drafted the manuscript; K.A.P. prepared the samples for electron microscopy; C.D.S. carried out the data collection on the samples; J.B.S. carried out the statistical analyses; A.P. provided assistance with the electron microscope; M.A.R., B.J. and P.R.H. contributed samples and helped draft the manuscript. All authors gave final approval for publication.

Competing interests. We declare we have no competing interests.

Funding. This work was supported by the National Institute of Neurological Disorders and Stroke at the National Institutes of Health (NS070717, NS042867 and NS073134), Eunice Kennedy Shriver National Institute of Child Health and Human Development (P30HD04067), National Science Foundation (BCS-1316829), and by the James S. McDonnell Foundation (220020293).

Acknowledgements. We thank that W. Andrew Barr for assistance creating figure 5.

References

1. Tomasch J. 1954 Size, distribution, and number of fibers in the corpus callosum. *Anat. Rec.* **119**, 119–135. (doi:10.1002/ar.1091190109)
2. Waxman SG. 1975 Integrative properties and design principles of axons. *Int. Rev. Neurobiol.* **18**, 1–40. (doi:10.1016/S0074-7742(08)60032-X)
3. Aboitiz F. 1992 Brain connections: interhemispheric fiber systems and anatomical brain asymmetries in humans. *Brain Res.* **25**, 51–61.

4. Ringo JL, Doty RW, Demeter S, Simard PY. 1994 Time is of the essence: a conjecture that hemispheric specialization arose from interhemispheric conduction delay. *Cereb. Cortex* **4**, 331–343. (doi:10.1093/cercor/4.4.331)
5. Aboitiz F, Scheibel AB, Fisher RS, Zaidel E. 1992 Fiber composition of the human corpus callosum. *Brain Res*. **598**, 143–153. (doi:10.1016/0006-8993(92)90178-C)
6. Witelson SF. 1989 Hand and sex differences in the isthmus and genu of the human corpus callosum. *Brain* **112**, 799–835. (doi:10.1093/brain/112.3.799)
7. Highley JR, Esiri MM, McDonald B, Cortina-Borja M, Herron BM, Crow TJ. 1999 The size and fibre composition of the corpus callosum with respect to gender and schizophrenia: a post-mortem study. *Brain* **122**, 99–110. (doi:10.1093/brain/122.1.99)
8. Caminiti R, Ghaziri H, Galuske R, Hof PR, Innocenti GM. 2009 Evolution amplified processing with temporally dispersed slow neuronal connectivity in primates. *Proc. Natl. Acad. Sci. USA* **106**, 19 551–19 556. (doi:10.1073/pnas.0907655106)
9. Tomasi S, Caminiti R, Innocenti GM. 2012 Areal differences in diameter and length of corticofugal projections. *Cereb. Cortex* **22**, 1464–1472. (doi:10.1093/cercor/bhs011)
10. Hopkins WD, Pilger JF, Storz R, Ambrose A, Hof PR, Sherwood CC. 2012 *Planum temporale* asymmetries correlate with corpus callosum axon fiber density in chimpanzees (*Pan troglodytes*). *Behav. Brain Res*. **234**, 248–254. (doi:10.1016/j.bbr.2012.06.030)
11. Hursh JB. 1939 Conduction velocity and diameter of nerve fibers. *Am. J. Physiol*. **127**, 131–139.
12. Gasser HS, Grundfest H. 1939 Axon diameters in relation to the spike dimensions and the conduction velocity in mammalian A fibers. *Am. J. Physiol*. **127**, 393–414.
13. Rushton WAH. 1951 A theory on the effects of fibre size in medullated nerve. *J. Physiol.* (*Lond.*) **115**, 101–122. (doi:10.1113/jphysiol.1951.sp004655)
14. Ritchie JM. 1995 Physiology of axons. In *The axon: structure, function, and pathophysiology* (eds SG Waxman, JD Kocsis, PK Stys), pp. 68–96. New York, NY: Oxford University Press.
15. Pajevic S, Basser PJ, Fields RD. 2014 Role of myelin plasticity in oscillations and synchrony of neuronal activity. *Neuroscience* **276**, 135–147. (doi:10.1016/j.neuroscience.2013.11.007)
16. Wang SS-H. 2008 Functional trade-offs in white matter axonal scaling. *Brain. Behav. Evol*. **72**, 159–167.
17. LaMantia AS, Rakic P. 1990 Axon overproduction and elimination in the corpus callosum of the developing rhesus monkey. *J. Neurosci*. **10**, 2156–2175.
18. Swadlow HA, Waxman SG, Geschwind N. 1980 Small-diameter non-myelinated axons in the primate corpus callosum. *Arch. Neurol*. **37**, 114–115. (doi:10.1001/archneur.1980.00500510072016.)
19. Caminiti R, Carducci F, Piervincenzi C, Battaglia-Mayer A, Confalone G, Visco-Comandini F, Pantano P, Innocenti G. 2013 Diameter, length, speed, and conduction delay of callosal axons in macaque monkeys and humans: comparing data from histology and magnetic resonance imaging diffusion tractography. *J. Neurosci*. **33**, 14501–14511. (doi:10.1523/JNEUROSCI.0761-13.2013)
20. Putnam MC, Steven MS, Doron KW, Riggall AC, Gazzaniga MS. 2010 Cortical projection topography of the human splenium: hemispheric asymmetry and individual differences. *J. Cogn. Neurosci*. **22**, 1662–1669. (doi:10.1162/jocn.2009.21290)
21. Wang SS-H, Shultz JR, Burish MJ, Harrison KH, Hof PR, Towns LC, Wagers MW, Wyatt KD. 2008 Shaping of white matter composition by biophysical constraints. *J. Neurosci*. **28**, 4047–4056.
22. Arnold C, Matthews LJ, Nunn CL. 2010 The 10 k trees website: a new online resource for primate phylogeny. *Evol. Anthropol*. **19**, 114–118. (doi:10.1002/evan.20251)
23. Stephan H, Frahm HD, Baron G. 1981 New and revised data on volumes of brain structures in insectivores and primates. *Folia Primatol*. **35**, 1–29. (doi:10.1159/000155963)
24. Zilles K, Rehkämper G. 1988 The brain, with special reference to the telencephalon. In *Orang-utan biology* (ed. JH Schwartz), pp. 157–176. New York, NY: Oxford University Press.
25. Rilling JK, Insel TR. 1999 The primate neocortex in comparative perspective using magnetic resonance imaging. *J. Hum. Evol*. **37**, 191–223. (doi:10.1006/jhev.1999.0313)
26. Hofer S, Frahm J. 2006 Topography of the human corpus callosum revisited: comprehensive fiber tractography using diffusion tensor magnetic resonance imaging. *Neuroimage* **32**, 989–994. (doi:10.1016/j.neuroimage.2006.05.044)
27. Hofer S, Merbolt KD, Tammer R, Frahm J. 2007 Rhesus monkey and human share a similar topography of the corpus callosum as revealed by diffusion tensor MRI *in vivo*. *Cereb. Cortex* **18**, 1079–1084. (doi:10.1093/cercor/bhm141)
28. Rohlf FJ. 2001 Comparative methods for the analysis of continuous variables: geometric interpretations. *Evolution* **55**, 2143–2160. (doi:10.1111/j.0014-3820.2001.tb00731.x)
29. Olivares R, Montiel J, Aboitiz F. 2001 Species differences and similarities in the fine structure of the mammalian corpus callosum. *Brain Behav. Evol.* **57**, 98–105. (doi:10.1159/000047229)
30. Innocenti GM, Vercelli A, Caminiti R. 2014 The diameter of cortical axons depends on both the area of origin and target. *Cereb. Cortex* **24**, 2178–2188. (doi:10.1093/cercor/bht070)
31. Aboitiz F, Montiel J. 2003 One hundred million years of interhemispheric communication: the history of the corpus callosum. *Braz. J. Med. Biol. Res*. **36**, 409–420. (doi:10.1590/S0100-879X2003000400002)
32. Buzsáki G, Logothetis N, Singer W. 2013 Scaling brain size, keeping timing: evolutionary preservation of brain rhythms. *Neuron* **80**, 751–764. (doi:10.1016/j.neuron.2013.10.002)
33. Perge JA, Niven JE, Mugnaini E, Balasubramanian V, Sterling P. 2012 Why do axons differ in caliber? *J. Neurosci.* **32**, 626–638. (doi:10.1523/JNEUROSCI.4254-11.2012)
34. Schmidt KE, Lomber SG, Innocenti GM. 2010 Specificity of neuronal responses in primate visual cortex is modulated by interhemispheric corticocortical input. *Cereb. Cortex* **20**, 2776–2786. (doi:10.1093/cercor/bhq024)
35. Dougherty RF, Ben-Shachar M, Deutsch G, Potanina P, Bammer R, Wandell BA. 2005 Occipital-callosal pathways in children validation and atlas development. *Ann. NY Acad. Sci.* **1064**, 98–112. (doi:10.1196/annals.1340.017)
36. Saenz M, Fine I. 2010 Topographic organization of V1 projections through the corpus callosum in humans. *Neuroimage* **52**, 1224–1229. (doi:10.1016/j.neuroimage.2010.05.060)
37. Hofman MA. 2014 Evolution of the human brain: when bigger is better. *Front. Neuroanat*. **8**, 15. (doi:10.3389/fnana.2014.00015)
38. Ghazanfar AA, Eliades SJ. 2014 The neurobiology of primate vocal communication. *Curr. Opin. Neurobiol*. **28**, 128–135. (doi:10.1016/j.conb.2014.06.015)